

In situ investigation of annealing effect on lamellar stacking structure of polyethylene thin films by synchrotron grazing-incidence small-angle and wide-angle X-ray scattering

Sono Sasaki,^{a*} Hiroyasu Masunaga,^a Hiroo Tajiri,^a Katsuaki Inoue,^a Hiroshi Okuda,^b Hiromichi Noma,^c Kohji Honda,^c Atsushi Takahara^d and Masaki Takata^{a,e}

^aJapan Synchrotron Radiation Research Institute / SPring-8, Hyogo 679-5198, Japan, ^bInternational Innovation Center, Kyoto University, Kyoto 606-8501, Japan, ^cGraduate School of Engineering, Kyushu University, Fukuoka 812-8581, Japan, ^dInstitute for Materials Chemistry and Engineering, Kyushu University, Fukuoka 812-8581, Japan, and ^eThe RIKEN Harima Institute / SPring-8, Hyogo 679-5198, Japan. Correspondence e-mail: sono@spring8.or.jp

We have investigated lamellar stacking structure of melt-crystallized and annealed high-density polyethylene (HDPE) thin films, with a thickness of *ca* 400 nm prepared on silicon wafers, using synchrotron grazing-incidence small-angle and wide-angle X-ray scattering (GISWAXS) measurements at the BL40B2 beamline in SPring-8. *In-situ* measurements of GISWAXS were carried out for the films in a stepwise annealing process under vacuum. Scattering peaks relating to the long period, the average distance between stacked crystalline lamellae, were measured only in the in-plane direction near the Yoneda peak of the grazing-incidence small-angle X-ray scattering patterns. On the other hand, the orthorhombic (110) and (200) reflections of oriented HDPE crystals were measured in the out-of-plane direction of the grazing-incidence wide-angle X-ray scattering patterns. It was revealed that crystalline lamellae were stacked in a parallel direction to the film surface and the long period increased from *ca* 25 nm to *ca* 32 nm in a stepwise annealing process. Within a lamella, molecular chains were found to be packed regularly and the chain axis (the *c* axis) was relatively oriented parallel to the film surface.

© 2007 International Union of Crystallography
Printed in Singapore – all rights reserved

1. Introduction

Polymer thin films have been used for parts of components of displays, insulation layers of semiconductors, materials to coat papers for printing and so on and their utilization and appreciation have been expanding in many kinds of industries. In order to control physical properties of polymer thin films, structural information peculiar for polymers confined to such narrow space should be revealed on molecular and meso scales. In general, crystalline polymers form higher-order structure consisting of crystal, amorphous and their intermediate regions. Meso-scale structure as to lamellar aggregation state in thin films has been investigated morphologically in their local area by transmission electron microscopy and atomic force microscopy. However, the average structural information on the long period, lamellar orientation and lamellar thickness have not been reported for the thin films at all.

It is well known that polymer chains in the solid state are reorganized from the initial structure to thermally more stable ones by annealing at various temperatures below the melting point. For example, defect concentration decreases and stress relief occurs in the crystal region of polymers. Also, partial melting and recrystallization

happen in the crystal and amorphous regions. We have reported crystallographic lattice dimension and distortion in the near-surface and bulk regions of melt-crystallized and annealed crystalline polymer thin films prepared on silicon wafers by grazing-incidence X-ray diffraction measurements (Yakabe *et al.*, 2004; Yakabe *et al.*, 2005). For a deep understanding of the annealing effect on crystalline polymer thin films, it is important to reveal lamellar-scale structural change.

The grazing-incidence small-angle X-ray scattering (GISAXS) method has lately attracted considerable attention as a powerful tool for the meso-scale structural analysis for thin films of polymers, for example, microphase-separated block copolymers and nanoporous polymers. GISAXS analysis based on distorted-wave Born approximation (DWBA) theory was applied for various multi-layer systems consisting of these films and substrates (Müller-Buschbaum *et al.*, 2004; Xu *et al.*, 2004; Tang *et al.*, 2005; Lee *et al.*, 2005; Park *et al.*, 2005; Chung *et al.*, 2006). In this study, we have tried to detect grazing-incidence small-angle and wide-angle X-ray scattering (GISWAXS) from crystalline polymer thin films. The lamellar aggregation structure of the thin films was investigated by combining these GISWAXS data. The annealing effect on lamellar stacking structure in poly-

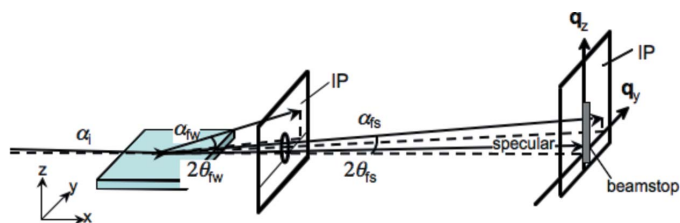


Figure 1
Schematic geometry of GISWAXS measurements: α_i is the incident angle of X-ray beams, α_s is the exit angle and $2\theta_i$ is the angle between the scattered beam and the plane of incidence. The subscripts s and w indicate GISAXS and GIWAXS geometries, respectively.

ethylene thin films prepared on silicon wafers has been investigated on molecular and meso scales by synchrotron GISWAXS measurements.

2. Experimental

The sample used in this study was an additive-free high-density polyethylene (HDPE, melt index = 14) supplied by Mitsui Chemicals, Inc., which is a typical example of crystalline polymers. Thin films of thickness of *ca* 400 nm were prepared onto the native oxide covered Si(110) surface of wafers with a 0.1 wt% *p*-xylene solution of HDPE under an N_2 atmosphere by a dip-coating method. The substrate was dipped into the solution heated at 373 K for 5 min, and then pulled out at the rate of 25 mm s^{-1} . The films obtained were isothermally crystallized at 373 K for 24 h from the melt under an N_2 atmosphere. Some of the melt-crystallized films were annealed at temperatures (T_a) of 378, 383, 388 or 393 K for 24 h under an N_2 atmosphere. The others were annealed at each T_a for 900 s in a stepwise heating process from 300 K to 453 K under vacuum.

In general, scattering from an organic thin film is relatively weak in intensity. Therefore, utilizing the high brilliance and highly parallel synchrotron X-rays as the incident beams is effective in detecting GISWAXS from HDPE thin films. In order to investigate the molecular- and meso-scale order structures of the films, synchrotron GISWAXS measurements were carried out with an imaging intensifier (II) and either a charge coupled device (CCD) detector or imaging plate (IP) detector at the BL40B2 beamline in SPring-8 (Hyogo, Japan). Fig. 1 shows experimental geometry of GISWAXS measurements. The components of the scattering vector, \mathbf{q} , parallel and perpendicular to the sample surface were defined as $q_y = (2\pi/\lambda)\sin(2\theta_i)\cos(\alpha_i)$ and $q_z = (2\pi/\lambda)[\sin(\alpha_i) + \sin(\alpha_s)]$, respectively, for reflected scattering. Here, α_i is the incident angle of X-ray beams, α_s is the exit angle, λ is the wavelength of incident X-ray beams and $2\theta_i$ is the angle between the scattered beam and the plane of incidence. The subscripts s and w in Fig. 1 indicate GISAXS and the grazing-incidence wide-angle X-ray scattering (GIWAXS) geometries, respectively. Nano-scale order structure such as chain-packing distance and chain orientation in the crystal region can be evaluated for the films by two-dimensional GIWAXS measurements. On the other hand, meso-scale order structure such as lamellar stacking distance and lamellar orientation can be investigated for the films on the basis of two-dimensional GISAXS data. The λ of incident X-rays was 0.15 nm and the sample-to-detector distances were *ca* 100 mm for GIWAXS and *ca* 2177 mm for GISAXS. A 2000 mm-length vacuum path was utilized between a sample cell and a detector for GISAXS measurements. Scattering patterns from the films were measured at α_i of 0.13 and 0.20°, which were lower and higher than the critical angle

of total external reflection at HDPE surface. The surface-sensitive scattering pattern was obtained for the films at α_i of 0.13°. The data collection time was 10 s per GISAXS pattern with the II and CCD detector and 300 s per GIWAXS or GISAXS pattern with the IP detector.

In-situ simultaneous measurements of GISWAXS were carried out for the films at T_a of 378, 383, 388 and 393 K in a stepwise annealing process from 310–453 K. The film on a silicon wafer was placed on a heater stage of a low-vacuum sample cell and sample temperature was accurately monitored and controlled with ultra-thin and wide K-type thermocouples and a program temperature controller. At each T_a , GISWAXS from the film was measured for 300 s after annealing it for 600 s. The heating rate was *ca* $10^\circ \text{ min}^{-1}$ and temperature fluctuation of the film at each T_a was $\pm 0.5^\circ$. Detectable \mathbf{q} -ranges of GIWAXS and GISAXS in these experiments were *ca* $21\text{--}4.2 \text{ nm}^{-1}$ and $1.3\text{--}4.2 \times 10^{-2} \text{ nm}^{-1}$, respectively.

3. Results and discussion

Figs. 2(a)–(f) show GIWAXS and GISAXS patterns measured at $\alpha_i = 0.13^\circ$ for a melt-crystallized HDPE thin film in the initial state at 310 K, in the stepwise annealed state at 378, 383, 388 and 393 K, and in the melt state at 453 K, respectively. As shown in the GIWAXS pattern in Fig. 2(a), the (110) and (200) reflections of oriented HDPE orthorhombic crystals were measured in the out-of-plane direction for the initial thin film. These reflections were azimuthally broad peaks and the intensity maximum of the (200) reflection was on the q_z axis. This indicates that the *a* axis of orthorhombic unit cell relatively oriented in the perpendicular direction to the film surface. In other words, the chain axis (the *c* axis) relatively oriented parallel to the film surface. The reflection peaks for annealed thin films were almost the same in q_y and q_z as those for the initial thin film. The relative intensity of these reflections increased with an increase in annealing temperature, as shown in the GIWAXS patterns of Figs. 2(b), 2(c), 2(d) and 2(e). This implied that the degree of crystallinity was

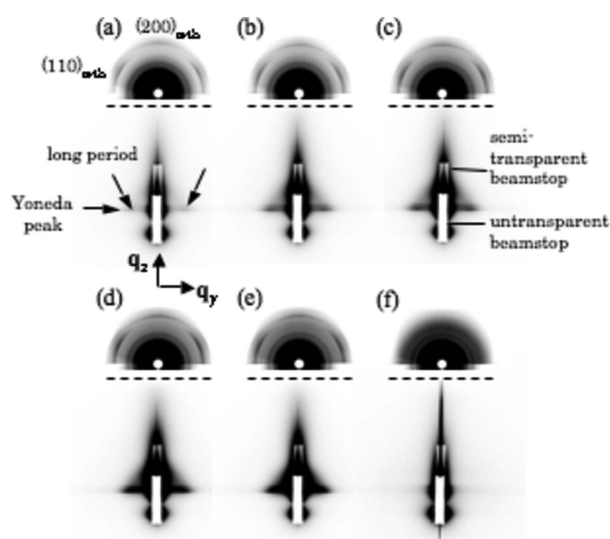


Figure 2
GIWAXS and GISAXS patterns measured at $\alpha_i = 0.13^\circ$ for a melt-crystallized HDPE thin film in the initial state at 310 K (a), in the stepwise annealed state at 378 K (b), 383 K (c), 388 K (d) and 393 K (e), and in the melt state at 453 K (f): the upper and lower images at each temperature are GIWAXS and GISAXS patterns, respectively. The untransparent and semi-transparent rectangular beamstops were connected to each other and used for GISAXS measurements.

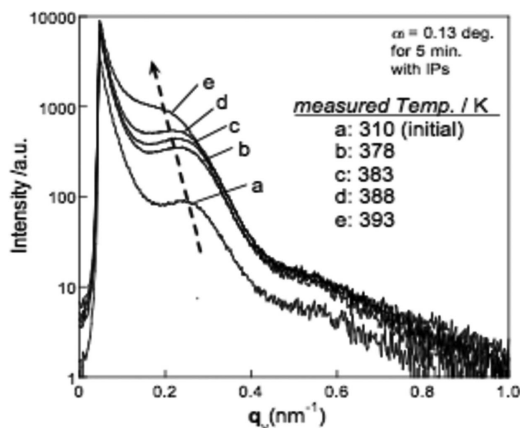


Figure 3
In-plane intensity profiles of the *in-situ* GISAXS patterns in Figs. 2(a)–(e) measured for the HDPE thin film in a stepwise annealing process from 310 K.

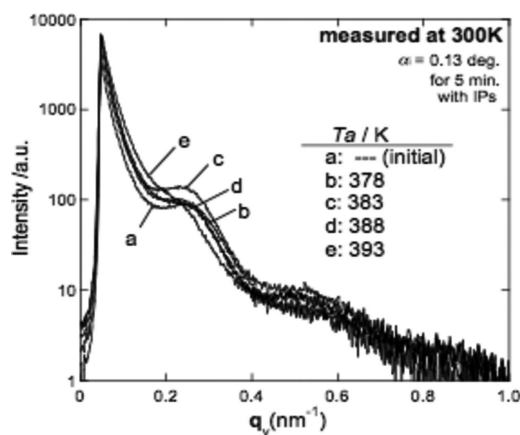


Figure 4
In-plane intensity profile of *ex-situ* GISAXS patterns measured for the melt-crystallized HDPE thin films at 300 K and those annealed individually at 378 K, 383 K, 388 K or 393 K for 24 h.

increased by annealing. The film was melted at 453 K, as shown the isotropic GIWAXS scattering pattern in Fig. 2(f).

On the other hand, scattering peaks were detected only in the in-plane direction near the Yoneda peak (Yoneda, 1963) in the pattern of Fig. 2(a), which means that crystalline lamellae were stacked in a parallel direction to the film surface. The q_y of these peaks relates to the long period, the average distance between stacked crystalline lamellae. The Yoneda peak arises in the in-plane direction owing to the interference effect of the incident and scattered wave (Chung *et al.*, 2006). By stepwise annealing, these scattering peaks slightly shifted to the lower q_y range in the in-plane direction and increased in relative intensity with an increase in T_a . The same tendency in Fig. 2 was obtained for GISWAXS patterns measured at $\alpha_i = 0.20^\circ$.

Fig. 3 shows in-plane intensity profiles of the *in-situ* GISAXS patterns at $\alpha_{fs} = 0.13 \text{ nm}^{-1}$ along the Yoneda peak in Figs. 2(a)–(e). It was clearly indicated that the shoulder peak gradually shifted from $q_y = ca 0.25 \text{ nm}^{-1}$ to $ca 0.20 \text{ nm}^{-1}$ with increasing sample temperatures from 310–393 K. Also, very weak and broad peaks observed around $q_y = ca 0.55 \text{ nm}^{-1}$ were considered to be the second-order peak of the above-mentioned strong scattering. The GISAXS data suggested that crystalline lamellae were stacked with large disordering in a parallel direction to the film surface and the long period became longer from $ca 25 \text{ nm}$ to $ca 32 \text{ nm}$ by annealing. Fig. 4 shows in-plane intensity profiles of *ex-situ* GISAXS patterns measured for

the melt-crystallized HDPE thin films at 300 K and those annealed individually at 378, 383, 388 or 393 K for 24 h. The peaks of the GISAXS profiles measured for the original thin film shifted slightly to a smaller q_y range by annealing, so that the long period became longer from $ca 25 \text{ nm}$ to $ca 27 \text{ nm}$. The long period estimated from the *in situ* profile in Fig. 3 was larger at 393 K than that from the *ex situ* profile in Fig. 4, which might be due to thermal expansion of stacked lamellae. It was suggested that the present experimental technique could cover the *in-situ* whole structure change of polymer thin films from meso to molecular scale. The two-dimensional GISAXS patterns will be simulated with a stacked lamellar model and the four different wavevector transfers induced the refraction-reflection phenomena.

4. Conclusions

We could successfully investigate lamellar stacking structure of melt-crystallized and annealed HDPE thin films prepared on silicon wafers by *in-situ* synchrotron GISWAXS measurements. Annealing effect on nano and meso-scale order structures of the thin films was clarified by the *in-situ* simultaneous measurement of GISAXS and GIWAXS. The GISWAXS data indicated that crystalline lamellae of the melt-crystallized HDPE thin film were stacked in a parallel direction to the film surface with the long period of $ca 25 \text{ nm}$. In a lamella, HDPE chains were regularly packed and the chain axis (the orthorhombic c axis) was relatively oriented parallel to the film surface. By stepwise annealing below the melting point, the long period was gradually increased to $ca 32 \text{ nm}$. Also, the degree of crystallinity might be increased without obvious change of the chain and lamellar orientation. The details of lamellar aggregation state will be investigated through simulating GISWAXS patterns in our future researches.

The authors would like to thank Dr H. Yakabe for his great help in film preparation. The synchrotron radiation experiments were performed at the BL40B2 beamline in SPRING-8 with the approval of the Japan Synchrotron Radiation Research Institute (JASRI) (Proposal No.: 2005B0655 and 2006A1212).

References

- Chung, B., Choi, M., Ree, M., Jung, J. C., Zin, W. C. & Chang, T. (2006). *Macromolecules*, **39**, 684–689.
- Lee, B., Oh, W., Hwang, Y., Park, Y.-H., Yoon, J., Jin, K. S., Heo, K., Kim, J., Kim, K.-W. & Ree, M. (2005). *Adv. Mater.* **17**, 696–701.
- Lee, B., Oh, W., Yoon, J., Hwang, Y., Kim, J., Landes, B. G., Quintana, J. P. & Ree, M. (2005). *Macromolecules*, **38**, 8991–8995.
- Lee, B., Park, Y.-H., Hwang, Y.-T., Oh, W., Yoon, J. & Ree, M. (2005). *Nature Mater.* **4**, 147–150.
- Lee, B., Park, I., Yoon, J., Park, S., Kim, J., Kim, J., Kim, K.-W., Chang, T. & Ree, M. (2005). *Macromolecules*, **38**, 4311–4323.
- Lee, B., Yoon, J., Oh, W., Hwang, Y., Heo, K., Jin, K.-S., Kim, J., Kim, K.-W. & Ree, M. (2005). *Macromolecules*, **38**, 3395–3405.
- Müller-Buschbaum, P., Hermsdorf, N., Roth, S. V., Wiedersich, J., Cunis, S. & Gehrke, R. (2004). *Spectrochem. Acta*, **B59**, 1789–1797.
- Park, I., Lee, B., Ryu, J., Im, K., Yoon, J., Ree, M. & Chang, T. (2005). *Macromolecules*, **38**, 10532–10536.
- Tang, C., Tracz, A., Kruk, M., Zhang, R., Smilgies, D.-M., Matyjaszewski, K. & Kowalewski, T. (2005). *J. Am. Chem. Soc.* **127**, 6918–6919.
- Xu, T., Goldbach, J. T., Minster, M. J., Kim, S., Gibaud, A., Gang, O., Ocko, B., Guarini, K. W., Black, C. T., Hawker, C. J. & Russell, T. P. (2004). *Macromolecules*, **37**, 2972–2977.
- Yakabe, H., Sasaki, S., Sakata, O., Takahara, A. & Kajiyama, T. (2004). *Trans. Mater. Res. Soc. Jpn.* **29**, 251–254.
- Yakabe, H., Tanaka, K., Nagamura, T., Sasaki, S., Sakata, O., Takahara, A. & Kajiyama, T. (2005). *Polym. Bull.* **53**, 213–222.
- Yoneda, Y. (1963). *Phys. Rev.* **131**, 2010–2013.